Optimization of Heavy Oil Upgrading using Dispersed Nanoparticulate Iron Oxide as a Catalyst

Almarshed, Abdullah; Hart, Abarasi; Leeke, Gary; Greaves, Malcolm; Wood, Joseph

DOI:
10.1021/acs.energyfuels.5b01451

energy&fuels

Article

pubs.acs.org/EF

Optimization of Heavy Oil Upgrading Using Dispersed Nanoparticulate Iron Oxide as a Catalyst

Abdullah Al-Marshed,[†] Abarasi Hart,[†] Gary Leeke,[†] Malcolm Greaves,[‡] and Joseph Wood*[,†]

[†]School of Chemical Engineering, University of Birmingham, Edgbaston, Birmingham B15 2TT, United Kingdom

[‡]IOR Research Group, Department of Chemical Engineering, University of Bath, Bath BA2 7AY, United Kingdom

ABSTRACT: It has previously been shown that *in situ* upgrading of heavy oil by toe-to-heel air injection (THAI) can be augmented by surrounding the horizontal production well with an annulus of pelleted catalyst. Despite the further upgrading achieved with this configuration, the accumulation of coke and metals deposits on the catalyst and pore sites, resulting from cracking of the heavy oil, have a detrimental effect on the catalyst activity, life span, and process. An alternative contacting pattern between the oil and nanoparticulate catalysts was investigated in this study, to mitigate the above-mentioned challenges. The Taguchi method was applied to optimize the effect of reaction factors and select the optimum values that maximize level of heavy oil upgrading while suppressing coke yield. The reaction factors evaluated were reaction temperature, H_2 initial pressure, reaction time, iron metal loading and speed of mixing. An orthogonal array, analysis of mean of response, analysis of mean signal-to-noise ratio (S/N) and analysis of variance (ANOVA) were employed to analyze the effect of these reaction factors. Detailed optimization of the reaction conditions with iron oxide dispersed nanoparticles ($\leq$50 nm) for *in situ* catalytic upgrading of heavy oil was carried out at the following ranges; temperature 355−425 °C, reaction time 20−80 min, agitation 200−900 rpm, initial hydrogen pressure 10−50 bar, and iron metal loading 0.03−0.4 wt %. It was found that the optimum combinations of reaction factors are temperature 425 °C, initial hydrogen pressure 50 bar, reaction time 60 min, agitation 400 rpm and iron−metal loading 0.1 wt %. The properties of upgraded oil at the optimum condition are API gravity 21.1°, viscosity 105.75 cP, sulfur reduced by 37.54%, metals (Ni+V) reduced by 68.9%, and naphtha plus middle distillate fractions (IBP: 343 °C) increased to 68 wt % relative to the feed oil (12.8° API, 1482 cP, sulfur content 3.09 wt %, metals (Ni+V) content 0.0132 wt %, and naphtha plus middle distillate fractions 28.86 wt %).

1. INTRODUCTION

Global fuel demand rises steadily as a result of ever-growing populations and developing economy. The trend in recent years has shown that the amount of conventional crude reserves available worldwide is in decline, which has been offset by the increasing exploitation of heavy crude oils and bitumen.[1,2] Although the former meet refinery feedstock specification, the latter requires upgrading to meet refinery specifications as well as to increase the yield of fuel fractions. This is because heavy oil and bitumen are characterized by high asphaltene, high viscosity, dense and low API (American Petroleum Institute) gravity, high heteroatom (e.g., sulfur, nitrogen, and oxygen), and metals content (e.g., nickel, iron, and vanadium).

The physicochemical properties of the heavy oil, bitumen or oil sands influence the choice of extraction technology. To this end, thermal enhanced oil recovery techniques such as steam assisted recovery and also *in situ* combustion is employed. *In situ* combustion methods involve combustion of a small portion of the oil in place to mobilize the rest through the heat released from the combustion reactions, which reduces the viscosity of the remaining oil and allows it to flow to a producer well. High temperatures up to 450−700 °C can be obtained in the reservoir, thereby promoting pyrolysis and *in situ* upgrading. The catalytic upgrading process *in situ* (CAPRI) is a technique to boost further the upgrading arising from the pyrolysis of heavy oil.[3] The concept is achieved in conjunction with toe-to-heel air injection (THAI). CAPRI is composed of a layer of catalyst packed into an annulus around the horizontal production well.[4,5]

Extraction and *in situ* upgrading offers the prospect of both enhancing recovery, and decreasing cost for a surface upgrading facility. *In situ* catalytic upgrading involves the use of the reservoir as a reactor, which offers cost, energy, and environmental benefits as it utilizes heat energy from *in situ* combustion to drive the catalysis, most of the impurities such as sulfur, vanadium, iron, and nickel are left behind in the reservoir, thus lowering the environmental footprint and impact on downstream refining processes, and reducing the cost of diluents to improve pipeline transport.[1,6,7] The usual configuration of the THAI−CAPRI process involves the packing of pelleted hydrotreating (HDT) catalysts around the perimeter of the horizontal production well.[5] However, in these studies, it was found that the catalyst loses its activity (i.e., deactivates) during reactions due to poisoning of active sites by impurities and blocking of pores induced by coke and metal deposition resulting from cracking of heavy oil.[4,8,9] Hence, attention has been shifted toward ultradispersed catalyst prepared *in situ* or injected as slurry into the reservoir to promote *in situ* catalysis during the THAI process. This is a once-through process.

Ultradispersed *in situ* catalytic upgrading has been reported to outperform the augmented catalytic upgrading achieved by incorporating pelleted refinery catalyst to the horizontal production well of the THAI process.[10−12] Using ultrafine

Received: June 29, 2015
Revised: August 11, 2015
Published: August 31, 2015

DOI: 10.1021/acs.energyfuels.5b01451
Energy Fuels 2015, 29, 6306−6316

Table 1. Properties of THAI Feedstock

properties	results	units
density @ 25 °C	0.9776	(g/cm^3)
API° gravity @ 15 °C	12.8	
dynamic viscosity @ 20 °C	1482	(cP)
asphaltene content	14	(wt %)
elemental analysis		
C	84.72	(wt %)
H	10.77	(wt %)
N	0.08	(wt %)
S	3.09	(wt %)
Ni	0.003	(wt %)
V	0.0102	(wt %)
(Ni+V)	0.0132	(wt %)
simulate distillation ASTM D2887		
naphtha fraction (initial boiling point, IBP: 177 °C)	0.68	(wt %)
distillate fraction (177−343 °C)	28.18	(wt %)
gas oil fraction (343−525 °C)	71.6	(wt %)

particles and pelleted Co−Mo/Al_2O_3 catalyst at reaction temperature 425 °C, the API gravity and viscosity of the produced oil was found to improve by respectively 9° API and 96% viscosity reduction with ultrafine particles compared to 5° API and 79% viscosity reduction achieved with pelleted fixed-bed catalyst.[10] Similarly, Ovalles et al.[13] showed that iron dispersed catalyst upgraded Hamaca extra-heavy oil from 500 to 1.3 Pa·s viscosities, 14% sulfur content reduction, and 41% conversion of >500 °C fraction relative to the original oil at 420 °C, 11 MPa, and a residence time of 1 h using a stirred batch reactor. As the size of particle decreases to nanoscale, its specific surface area increases while the diffusion path length decreases, this improves interaction with macromolecules and cracking reaction. Also, the nanoparticles (NPs) experience lower interparticle distances that increase the probability of active phase interaction with the hydrocarbon molecules.

Compared to HDT catalysts such as Ni−Mo/Al_2O_3 and Co−Mo/Al_2O_3, NPs of iron oxide (Fe_2O_3) are potentially cost-effective as the ore hematite (α-Fe_2O_3) is one of the most abundant iron oxide minerals and also nontoxic.[14] Additionally, nanoparticles of iron oxide do not require rigorous and special methods of preparation. Iron NPs can readily be separated using magnetic separation. Adding silica (SiO_2) and maghemite (γ-Fe_2O_3) NPs to *in situ* combustion substantially increases fuel distillates produced and decreases the activation energies of the thermocatalytic conversion of heavy oil.[15] In this study, a comprehensive optimization of the iron dispersed NPs for *in situ* upgrading during the THAI process was carried out in a stirred batch reactor. Investigations include the effects of reaction temperature, iron metal loading, reaction time, mixing, and initial hydrogen pressure on the extent of upgrading in terms of API gravity increase, viscosity reduction, asphaltene content, sulfur and metals reduction, and true boiling point (TBP) distribution. The impact of these variables on the yields of liquid (i.e., upgraded oil), gas, and coke after reaction was also explored. This optimization is to maximize the upgrading in the produced oil while suppressing coke formation. The Taguchi method was used to analyze statistically the data and optimize the signal-to-noise ratio.[16]

2. MATERIALS AND METHODS

2.1. Feedstock and Catalyst. A heavy crude sample was supplied from the Whitesands THAI pilot trial, Conklin, Alberta, Canada by Petrobank Energy and Resources Ltd. The crude oil sample was partially upgraded during the thermal recovery stage of the THAI process and consists of a mixture of partially upgraded crude produced from eight different wells. The chemical and physical properties of the crude sample was measured and presented in Table 1. The iron(III) oxide (Fe_2O_3) nanoparticles (NPs) used in the experiments were purchased from Sigma-Aldrich, United Kingdom, and their properties are thus: density 5.24 g·cm^{-3} and particle size less than 50 nm.

2.2. Experimental Apparatus. Studies to determine the effect of reaction factors on heavy oil upgrading as well as optimization of the several reaction factors were carried out in a stirred batch reactor (100 mL capacity, Baskerville UK). The batch reactor enabled the screening of an economical quantity of iron NPs and oil while exercising proper control. Prior to startup, the reactor was pressurized with hydrogen to an initial pressure (i.e., 10, 25, 40, and 50 bar), which increased to about 70 bar when initial hydrogen pressure of 50 bar, with the rising temperature and gas expansion and production due to cracking reactions. The high pressures generated signify that the process is appropriate for reservoir depths greater than 75 m. Once the desired temperature is reached, the appropriate reaction time was allowed. A detailed description of the experimental procedure has been reported elsewhere.[10] The oxide form of the iron nanoparticles is converted to a sulfide form during the reaction because of the sulfur rich heavy feed.[17]

2.3. Taguchi Method. The Taguchi method used in this study to optimize the reaction factors has been reported in detail elsewhere.[16,18] The following variables reaction temperature (°C), H_2 initial pressure (bar), reaction time (min), iron metal loading (wt %), and mixing speed (rpm) were selected as controllable factors, and their levels investigated are shown in Table 2.

Table 2. Selected Controllable Factors and Their Levels

	control level			
factors	Level 1	Level 2	Level 3	Level 4
reaction temperature (°C)	355	370	395	425
initial H_2 pressure (bar)	10	25	40	50
reaction time (min)	20	40	60	80
iron metal Loading (wt %)	0.03	0.06	0.1	0.4
mixing speed (rpm)	200	400	600	900

An orthogonal array was formed based on the Taguchi method to generate the number of experiments to examine the effect of different controllable factors, with each factor having a different level.[19] In this study, five controllable factors and four levels were formed (see Table 2) and the proper orthogonal array is L16 presented in Table 3. The details on how to select standard orthogonal array were reported in the literature.[16,20−22]

DOI: 10.1021/acs.energyfuels.5b01451
Energy Fuels 2015, 29, 6306−6316

Table 3. Orthogonal Array Used To Determine Experimental Conditions That Were Tested in the Upgrading Experiment

	reaction factors				
experiment number	reaction temperature (°C)	initial H_2 pressure (bar)	reaction time (min)	iron metal loading (wt %)	speed of mixing (rpm)
1	355	10	20	0.03	200
2	355	25	40	0.06	400
3	355	40	60	0.1	600
4	355	50	80	0.4	900
5	370	10	40	0.1	900
6	370	25	20	0.4	600
7	370	40	80	0.03	400
8	370	50	60	0.06	200
9	395	10	60	0.4	400
10	395	25	80	0.1	200
11	395	40	20	0.06	900
12	395	50	40	0.03	600
13	425	10	80	0.06	600
14	425	25	60	0.03	900
15	425	40	40	0.4	200
16	425	50	20	0.1	400

The Taguchi method uses the signal-to-noise ratio (S/N) function to obtain the optimum conditions. The (S/N) is the ratio between the desired values of a response variable and the undesired values of a response variable.[20] The three main S/N ratios used for the selection of optimum conditions with their formulae are presented in Table 4.[20,23]

Table 4. Signal-to-Noise Ratio (S/N) Type and Application[a]

signal-to-noise ratio type	application	formula
smaller the better	minimum response variable	$\left(\frac{S}{N}\right) = -10\log\left(\frac{1}{n}\sum_{i=1}^{n} y_i^2\right)$
larger the better	maximum response variable	$\left(\frac{S}{N}\right) = -10\log\left(\frac{1}{n}\sum_{i=1}^{n} \frac{1}{y_i^2}\right)$
nominal the best		$\left(\frac{S}{N}\right) = -10\log\left(\frac{1}{n}\sum_{i=1}^{n} \frac{1}{\overline{y}_i^2}\right)$

[a]Where n, number of measured value; y_i^2, measured value; S^2, standard deviation; $\overline{y}^2$, mean square of measured value. Analysis of variance (ANOVA) is a statistical technique that is used percentage contribution to determine which variables have a significant influence upon heavy oil upgrading. Details of the ANOVA analysis can be found elsewhere.[22]

The (S/N) ratio is used to measure the quality characteristic of deviation from a desired variable and it should always be maximized in order to allow the response variable to approach optimum conditions.

2.4. Data Analysis. On the basis of the Taguchi method, the analysis was conducted in two parts, namely mean response analysis and mean signal-to-noise ratio analysis. As shown in Table 3, each experiment is a combination of different levels. To identify the main effect of each controllable factor, the Taguchi method suggests calculating the mean value of the measured response variable for the corresponding level setting.

2.5. Analysis of Products. The main products of the upgrading reactions are upgraded oil (i.e., liquid), noncondensable gas, and coke, quantified by mass balance. The mass balances of the two products gas and coke were calculated and reported as a percentage of the mass of oil fed using eq 1. The mass of gas produced was therefore calculated as the mass remaining after subtracting the masses of the upgraded oil and coke fractions in the reactor from the fed mass of THAI feedstock.

$$\text{yield (wt\%)} = \frac{m_i}{m_{\text{feedstock THAI}}} \times 100 \quad (1)$$

where m_i is weight of component i.

The following analysis was performed on the collected upgraded oil to quantify the extent of upgrading when compared with the original oil: Advanced rheometer AR 1000 (TA Instruments Ltd., United Kingdom) was used to measure the viscosity, Anton Paar DMA 35 density meter was used to quantify the density and API gravity, and simulated distillation by Agilent 6850N gas chromatography (GC) in line with ASTM D2887 method (the calibration mix of the GC contain hydrocarbons from C_5 to C_{40} and also the maximum oven temperature is 280 °C, hence the macromolecules such as resins and asphaltenes outside this carbon range cannot be accounted for) was used to obtain the true boiling point (TBP) distribution curve. The GC is fitted with a DB-HT 5 m length, 0.53 mm internal diameter, and 0.15 μm film thicknesses capillary column. It is also incorporated with a programmed temperature vaporization (PTV) injector that rapidly heats the sample to 360 °C to vaporize the sample prior to injection into the column. A detailed description of these instruments has been provided by Hart et al.[8] The sulfur and metal contents of the feedstock and the upgraded oil were determined by Warwick Analytical Service, United Kingdom, using inductively coupled plasma-optical emission spectroscopy (ICP-OES).

3. RESULTS AND DISCUSSION

Experiments in Table 3 were repeated three times. The samples were analyzed and pooled standard deviation were calculated to quantify the variance of the results as follows: coke wt % ±0.14, middle distillate wt % ±0.25, light naphtha wt % ±0.22, gases wt % ±0.46, API ±0.28°, viscosity ±0.5, sulfur wt % ±0.025, metal (Ni+V) wt % ±0.031.

Table 5. Dispersed Iron Metal Oxide Performance at Different Levels of Severity

catalysts	non[a]	Fe_2O_3[a]	non[b]	Fe_2O_3[b]	non[c]	Fe_2O_3[c]
product distribution						
coke (wt %)	2.21 ± 0.15	0.89 ± 0.1	7.73 ± 0.21	7.94 ± 0.31	12 ± 0.35	6.79 ± 0.11
gas (wt %)	5.73 ± 0.13	4.8 ± 0.1	8.7 ± 0.15	9.8 ± 0.2	12 ± 0.14	10.72 ± 0.2
SIMDIST boiling point distribution (wt %)						
(IBP: 177 °C)	17 ± 0.11	16 ± 0.16	23 ± 0.18	22 ± 0.21	25 ± 0.2	21 ± 0.3
(177−343 °C)	43 ± 0.44	44 ± 0.4	43 ± 0.2	45 ± 0.31	43 ± 0.14	47 ± 0.1
physical properties						
API gravity° @ 15 °C	19 ± 0.2	19 ± 0.3	22 ± 0.1	21 ± 0.1	24 ± 0.2	21 ± 0.1
viscosity (cP)	203.24 ± 1.7	217.61 ± 1	82.4 ± 1.4	112.03 ± 1	53.54 ± 2	105.75 ± 1.5

[a]Reaction conditions: one step (410 °C, 60 min, H_2 initial pressure 50 bar, mixing speed 900 rpm). [b]Reaction conditions: one step (425 °C, 60 min, H_2 initial pressure 50 bar, mixing speed 900 rpm). [c]Reaction conditions: two steps (410 °C, 50 min, H_2 initial pressure 50 bar, mixing speed 900 rpm followed by 425 °C, 60 min, mixing speed 900 rpm). Non = no catalyst.

DOI: 10.1021/acs.energyfuels.5b01451
Energy Fuels 2015, 29, 6306−6316

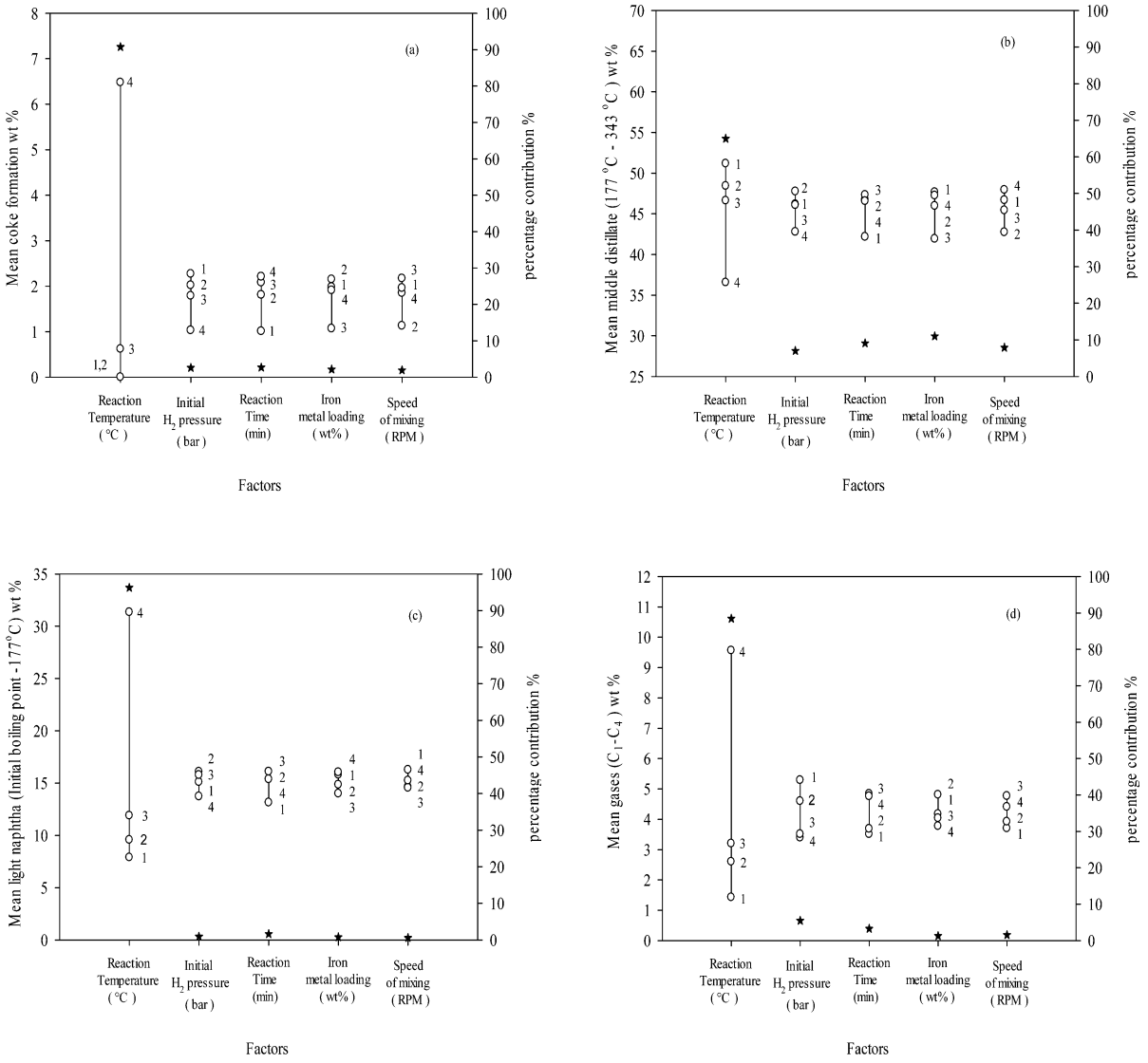

Figure 1. Effect of reaction factors on product distribution. (a) Mean coke formation wt %; (b) mean middle distillate (177−343 °C) wt %; (c) mean light naphtha (IBP: 177 °C) wt %; (d) mean gases (C_1−C_4) wt %. The mean of each factor is indicated by a circle, the number next to each circle indicates the factor level, and the percentage contribution is indicated by an asterisk. For details of reaction factors and their levels, see Table 2.

3.1. Catalyst Activity. Table 5 summarizes the performance of dispersed iron metal oxide (Fe_2O_3, size ≤50 nm) at different levels of reaction factors for liquid, gas and coke products.

It is clear from Table 5 (condition b) that dispersed iron metal oxide (Fe_2O_3) has very poor activity. This is because the results were very close to those obtained in the absence of catalyst (i.e., thermal cracking) at 425 °C. On the other hand, the catalyst has better activity in terms of inhibiting coke formation, as the coke observed was 60% below the 2.21 wt % coke yield for thermal reaction only. The results are consistent with the literature where similar observations were reported.[24−26]

The activation of dispersed catalysts can be achieved *in situ* due to the sulfidation reaction between the iron NPs and the sulfur contained in the heavy oil to generate active metal sulfide phase.[27] Though not reported here, the analysis of the spent NPs of iron showed pyrrhotite ($Fe_{1-x}S$), which is postulated to occur during the heating stage to the reaction temperature. The sulfidation of the iron NPs is also confirmed by the decreased sulfur content of the upgraded oil relative to the feed oil (discussed in Section 3.4). This process can influence the activity of the NPs as well as their upgrading performance. It has been reported that the activation of dispersed catalysts could be improved by carrying out a low reaction temperature step, consisting of catalyst reduction under a flow of hydrogen at milder temperature than the reaction itself, followed by high temperature reaction.[26−29] It was observed from Table 5 that the two-step experiment helped in improving the catalyst activity under more severe conditions (425 °C, 60 min) where the coke yield reduced from 12 wt % (thermal cracking) to 6.76 wt % (catalytic). In addition, the middle distillate production was increased to 47 wt % (catalytic) relative to the feedstock containing 28.18 wt %, which is in agreement with the literature.[26,29] Hence, the addition of iron NPs suppressed coke formation significantly while slightly improving product distribution relative to thermal cracking (Table 5, reaction condition c).

3.2. Effect of Reaction Factors on Product Distribution. Heavy oil upgrading is aimed at improving the yield of middle distillate fraction while gas and coke yields are inhibited.[30] The effects of reaction factors on product distribution are graphically

DOI: 10.1021/acs.energyfuels.5b01451
Energy Fuels 2015, 29, 6306−6316

presented (vertical point plot) in Figure 1. The value of the percentage contribution indicated on the second *y*-axis shows the extent of influence contributed by the reaction variable on the upgrading.

Qualitatively, Figure 1 shows that the formation of coke, light naphtha fraction (IBP: 177 °C), middle distillates fraction (177−343 °C), and gases (C_1−C_4) are highly affected by reaction temperature for all factors. The relationships between coke, light naphtha, and gas and reaction temperature are shown in Figure 1a,c,d, respectively. The coke, light naphtha fraction, and gas formation increases gradually at low reaction temperature Level 1 and 2 (355 and 375 °C, respectively). However, the increased rate of mean percentage weight of coke, light naphtha, and gas becomes greater at the high reaction temperature Level 4 (425 °C). The mean percentage weight of coke formation is negligible at Level 1 and Level 2 reaction temperature, and the coke started to form at an intermediate level where coke formation reached 0.62 wt % at Level 3 (395 °C), and it rises to its maximum value of 6.48 wt % at Level 4 reaction temperature. Furthermore, the mean percentage weights for light naphtha fraction (IBP: 177 °C) at the respective reaction temperatures are as follows: 7.88 wt % (Level 1), 9.57 wt % (Level 2), 11.89 wt % (Level 3), and 31.34 wt % (Level 4), relative to 0.67 wt % the light naphtha fraction in feed oil. A similar trend can be noticed in the mean of percentage weights of gases (C_1−C_4) 1.43% (Level 1), 2.6% (Level 2), 3.2% (Level 3), and 9.56% (Level 4) for reaction temperature. On the other hand, Figure 1b shows that the middle distillate fraction (177−343 °C) gradually decreases as the reaction temperature increases for Levels 1, 2, and 3. However, the decreasing rate of middle distillate fraction (216−343 °C) becomes faster at the high reaction temperature Level 4. The mean of percentage weights of the mean middle distillate fraction (177−343 °C) for reaction temperature can be summarized as 51.18 wt % (Level 1), 48.43 wt % (Level 2), 46.62 wt % (Level 3), and 36.56 wt % (Level 4) respectively, relative to 27.59 wt % (feed oil). Similar observations have been reported in the literature.[31,32] This is because as the reaction temperature increases, the cleavage of C−C and C−heteroatom bonds increases as well as condensation and polymerization reactions between free-radicals being favored, which are thought to be responsible for the high yield of light naphtha, gas, and coke.[10,26]

The results of experiments carried out at various levels of dispersed catalytic loading, reaction time, initial H_2 pressure, and speed of mixing are graphically presented in Figure 1a−d. It is clear that these factors do not exhibit as much effect as reaction temperature because the cleavage of C−C and C−heteroatom bonds are dependent on temperature. However, the chemistry of hydroconversion reactions can be enhanced by these factors.[30,33,34]

The produced coke, light naphtha, and gas appears to be inhibited slightly as H_2 initial pressure increased from Level 1 to Level 4 (10−50 bar) as shown in Figure 1a,c,d. As a consequence, the mean percentage weights of coke ranged from (2.27 to 1 wt %), light naphtha (16.27 to 13.73 wt %), and gas (5.29 to 3.5 wt %). Also, the production of middle distillate remained within a narrow range between 46 to 42 wt % as H_2 initial pressure change from Level 1 to Level 4, as shown in Figure 1b. This observation is consistent with the literature where it has been reported that at moderate reaction pressure (70 bar) the yield of light product and gas is reduced.[35] In other words, the intermediate fraction does not undergo secondary hydrocraking; hence, the produced gas and light fractions are mainly products of hydrocracking of the heavy fraction. In addition, the hydrogenation reaction could be expected to be more active at moderate pressure whereas at high pressure the hydrocracking dominates.[17,35,36]

In Figure 1a−d, the effect of reaction time is also presented. It is clear that the reaction time does not have as much impact as reaction temperature. However, a long reaction time promotes cracking, secondary cracking of intermediates and more yields of coke, light naphtha, middle distillate, and gas. The mean percentage weights of coke ranged from 1 to 2.2, middle distillate 42 to 46.5 wt %, light naphtha 13 to 16 wt %, and gas 3.5 to 5 wt % as the reaction time increased from Level 1 to Level 4 (20−80 min). The iron metal loading does not exact significant impact on inhibition of formation of coke, light naphtha and gas; however, the middle distillate fraction is stable even in the presence of low iron metal loading (Figure 1a−d). Notably, an increase in the iron metal loading from Level 1 to Level 3 (i.e., 0.03 to 0.1 wt %) led to a reduction in mean coke (1.5 wt %), light naphtha (1 wt %), and gas (2 wt %) after reaction. In addition, the mean percentage weights of the middle distillate fraction ranged from 42 to 47 wt % as the iron metal loading changed from Level 1 to Level 4. In comparison to supported catalysts, dispersed catalyst particles in heavy oil are less susceptible to deactivation during heavy oil upgrading. Dispersed NPs offer better contact with reactants than the supported pelleted catalysts, which may lead to an increased reaction surface area as well as reduced mass transfer limitations between reactants.[37,38] As particle size decreases its surface area increases, therefore dispersion offers the usage of the entire surface related to pelleted counterpart. The iron NPs is pure iron oxide; hence the active phase is dispersed on the external surface after sulfidation. The process of stabilizing free radicals should be rapid in the presence of active hydrogenation catalysts to avoid fast and undesirable condensation reactions that would lead to form the mesophase then coke, respectively.[26,39,40] The reduced coking observed can be attributed to the nanodispersed iron oxide catalysts and boosts hydrogen uptake during hydro-cracking reactions (see Figure 1a). This helped to control the rate of free radical propagation via β-scission reactions and subsequently to the conversion of heavy fractions to lighter products are improved.[41,42] These reaction stages are as follows:

initiation:

$$M \xrightarrow{k1} 2R^{\cdot}$$

propagation:

$$\text{chain transfer} \quad R^{\cdot} + M \xrightarrow{k2} RH + M^{\cdot}$$

$$\beta\text{-scission} \quad M^{\cdot} \xrightarrow{k3} R^{\cdot} + \text{olefin}$$

termination:

$$\text{radical} + \text{radical} \xrightarrow{k4} \text{product}$$

where M is the parent compound, and $R^{\cdot}$ is the smaller alkyl radical.

On the other hand, it was observed that at Level 4 (0.4 wt %) of iron metal loading the mean of percentage weights for products tended to again increase approximately for coke (1 wt %), gas (1 wt %), and light naphtha (3 wt %). These results show a similar trend in coke formation to dispersed MoS_2 catalyst.[43,44] However, the activity experienced with MoS_2 is higher compared to Fe_2O_3. It was suggested that a high level of active metal sulfide (MoS_2) could lead to a high level of hydrogenation that reduces asphaltene stability and promotes coke formation.[40,43]

DOI: 10.1021/acs.energyfuels.5b01451
Energy Fuels 2015, 29, 6306−6316

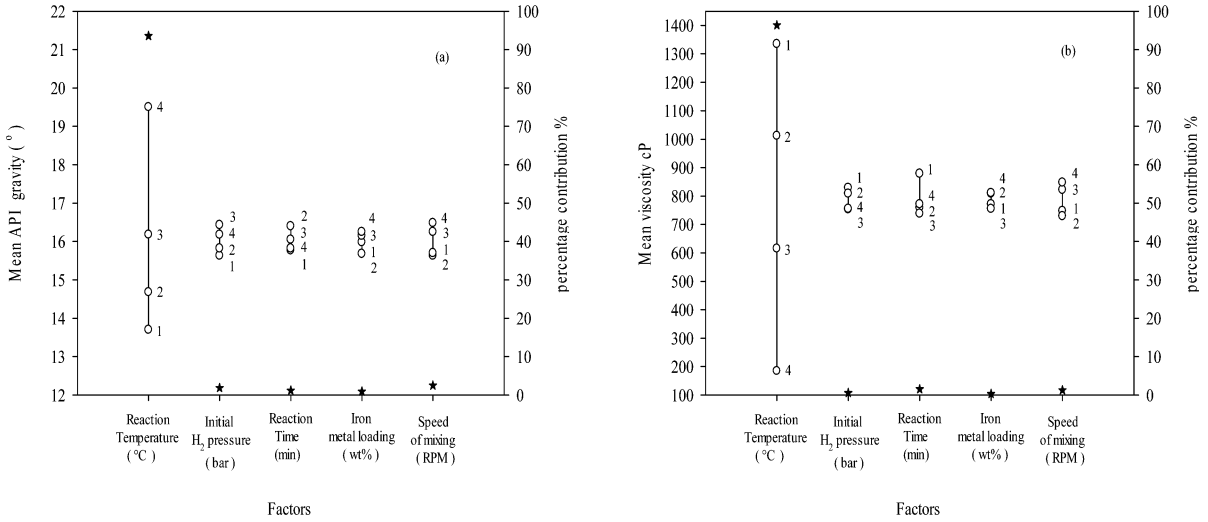

Figure 2. Effect of reaction factors on physical properties (a) mean API gravity (b) mean viscosity. The mean of each of the factors is indicated by a circle and the number next to each circle indicates the factor level, the percentage contribution indicated by an asterisk. For details of reaction factors and their levels, see Table 2.

The flow of oil over the dispersed nanoparticles will create some sort of mixing; hence, the effect of agitation upon the level of upgrading achieved was studied. It was observed that the levels of upgrading in terms of product distribution achieved at agitation speed of 200 rpm were 1.8 wt % (coke), 46 wt % (middle distillate), 16.26 wt % (light naphtha), and 3.7 wt % (gas). At 900 rpm mixing speed, the mean percentage weights were 1.9 wt % (coke), 47 wt % (middle distillate), 15.5 wt % (light naphtha), and 4.5 wt % (gas) (Figure 1a–d). Because the particle size is small dispersion can be achieved with minimal mixing speed; hence, minor changes were observed in the product distribution. These results are consistent with the literature where it has been reported that the yield of produced coke and gas is decreased during hydro-cracking of residue using nickel sulfate and ferrous sulfate as dispersed catalysts at the stirring rate 400–4000 rpm and reaction temperature 430 °C.[45] In comparison to noncatalytic (i.e., thermal) upgrading, the yields of coke and gas were reduced to 3.47 and 5.32 wt % respectively, relative to yields of 10.81% (coke) and 8.84% (gas) reported by Luo et al.[45] for thermal upgrading. Luo et al.[45] also reported that the yields of coke ranged from 3.47 to 3.03 wt %, whereas gas ranged from 5.23 to 3.81 wt % as the mixing speeds increased from 500 to 2000 rpm. In addition, the same study showed that yields of both coke and gas decrease slightly with changing loading of dispersed catalysts from 0.01 to 0.06 g·mL^{-1}.

An important step in the hydrocracking reaction is the saturation of free radicals, which is mainly promoted by hydrogenation catalysts.[46] In addition, the dispersion of catalysts and hydrogen gas could be improved by good mixing.[30,45,47] This explains why increased hydrogen pressure, increased iron metal loading, and good mixing suppressed coke and gas formation as well as improving middle distillate production even at high reaction temperatures (see Figure 1a–d).

3.3. Effect of Reaction Factors on Physical Properties.

The API gravity of the crude oil is one important factor for assessing the quality of crude oil. High crude oil viscosity is detrimental for extraction as well as pipeline transport. In addition, the high level of heavy oil upgrading is characterized in physical terms by an increase in the API gravity and when its dynamic viscosity is reduced by few orders of magnitude.[6] The viscosity and API gravity of the crude oil is greatly influenced by its macromolecular weight constituents, such as resins and asphaltenes; chemical composition can also play a major part.

Figure 2 shows the effect of reaction factors such as reaction temperature, reaction time, H_2 initial pressure, mixing, and iron metal loading on the produced oil API gravity and viscosity.

It is shown in Figure 2 that the API gravity of the produced oil increased as the reaction temperature increases from Level 1 to Level 4 (355 to 425 °C). The API gravity for the produced oil was 19.5° (Level 4) and 13.7° (Level 1), compared to 12.8° for the heavy feed oil. Correspondingly, the produced oil viscosity decreased as the reaction temperature increases (see Figure 2a,b). These trends in API gravity and viscosity with reaction temperature were expected as similar observations had been reported earlier in the literature.[1] This can be attributed to increased cracking reactions at a higher temperature, which is compounded by a corresponding increase in gas production and coke as the temperature increases. Hart et al.[8] reported a similar effect of temperature on the catalytic cracking of heavy oil.

The significant influence of reaction temperature increase on the API gravity and viscosity can be observed in Figure 2a,b. An increase in temperature accelerates the rate of the three major reactions occurring in the slurry environment such as (a) free-radical formation from C–C and C–heteroatom bonds cleavage, (b) hydrogen-transfer reactions (i.e., hydrogen-abstraction by C–H bond scissions and hydrogen-addition capping free-radicals), and (c) condensation and polymerization reactions between free-radicals.[1,42,48] However, in the absence of active catalysts and at reaction temperature above 420 °C, reactions with conditions a and c dominate. As a consequence of these reactions, lighter oil (high yield of light naphtha fraction), gas, and coke were observed. This is reflected in the observed increase in API gravity and decreased oil viscosity.[46]

An increased hydrogen pressure increases the availability of hydrogen for hydroconversion reactions,[35,49] but the oil API gravity and viscosity changes slightly with the initial pressure from Level 1 to Level 4 (10–50 barg). An average increase of 0.85° was observed for API gravity, whereas a change of 75.6 cP was observed in viscosity, respectively (Figure 2a,b). Hence, initial hydrogen pressure does not achieve as much effect on API gravity and viscosity as reaction temperature. Hart et al.[1] and Elizalde et al.[36] observed a similar effect of hydrogen pressure on

DOI: 10.1021/acs.energyfuels.5b01451
Energy Fuels 2015, 29, 6306–6316

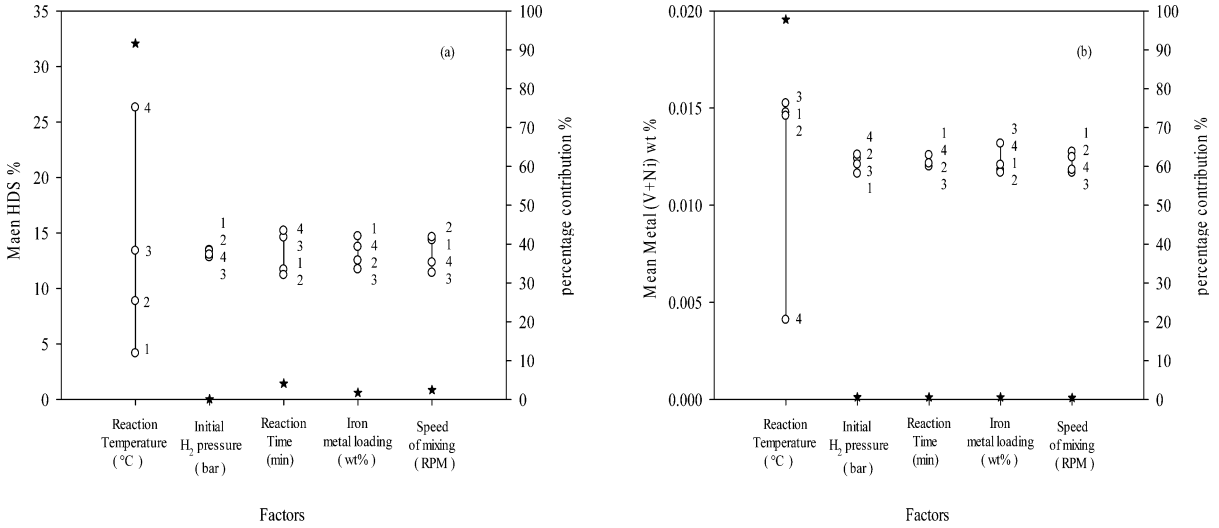

Figure 3. Effect of reaction factors on product quality (a) mean HDS % (b) mean metal (V+Ni) wt %. The mean of each factors is indicated by a circle and the number next to each circle indicates factor level, with percentage contribution indicated by an asterisk. For details of reaction factors and their levels, see Table 2.

API gravity and viscosity of the produced oil in fixed bed catalytic upgrading of heavy oil.

In Figure 2a,b, the effect of reaction time is presented. The API gravity of the produced oil increases from 15.8° to 16.4° API as the reaction time increased from Level 1 to Level 2 (20 to 40 min) and thereafter, the API decreased to 15.8° with further increase in reaction time from Level 3 to Level 4. Though the reaction time does not achieve as much impact as temperature, long reaction time promotes over cracking, secondary cracking of intermediates and a greater yield of coke, which contributed to the trend observed. Also, prolonged reaction time would have promoted condensation and polymerization reactions between free-radicals resulting in the formation of larger molecular weight product, which explains the low API gravity and slightly higher viscosity of the produced oil. The availability of active sites decreases with time as a result of adsorption of resins and asphaltene, coke, and metals deposits (i.e., deactivation of catalyst) and suppresses the performance of the dispersed NP catalyst and contributed also to the observed trend in API gravity and viscosity with reaction time.

It was observed that the value of API gravity decreased from 16.48° to 15.7° as the agitation speed varies from 200 to 900 rpm (Level 1 to Level 4). The viscosity was 747.6 cP at Level 1 (200 rpm) and increased to 847.4 cP at Level 4 (900 rpm). An increase in agitation could lead to enhanced nanoparticle dispersion and contacting of oil-solid within the reaction medium,[50] which will decrease the mass transfer barrier between the solid−liquid−gas and improve upgrading.[30] Nevertheless, an optimum API gravity and viscosity could be reached at agitation speeds from Level 2 to Level 4 (400−900 rpm). This could be attributed to nanosize particles, which required intermediate mixing speed to achieve adequate suspension necessary for reaction.[30,50] This is within the same range of agitation reported by Hart et al.,[10] who found an optimum at 500 rpm.

The iron metal is responsible for hydrogen activation and transfer reactions to moderate produced free radicals from the cracking of heavy molecules.[24] The iron metal loading does not have significant impact on the API gravity and viscosity of the produced oil (see Figure 2a,b) because it is unsupported (i.e., pure iron oxide) unlike bifunctional catalyst supported on zeolites and alumina promote C−C cleavage due to their acidic sites, rather the iron NPs support hydrogen transfer reactions. This means that lack of acidic site on the iron NPs impede cracking functionality.

Notably, an increase in the iron metal loading from Level 1 to Level 4 (i.e., 0.03 to 0.4 wt %) led to minor changes in API gravity and viscosity of the produced oil after reaction by 0.85° and 55.9 cP, respectively.

3.4. Effect of Reaction Factors on Product Quality. The high content of sulfur and metals (i.e., Ni and V) adversely impact on downstream processes such as catalytic reforming, hydrotreating and the cost of hydrotreatment. Hence, upgrading is also aimed at decreasing the level of impurity to meet refinery feedstock specification. Figure 3 shows the extent of sulfur and metals reduction for the different reaction factors.

From Figure 3a, as the reaction temperature increases from Level 1 to Level 4 (i.e., 355 to 425 °C), the extent of hydrodesulfurization (HDS) increases in that order from 4.2 to 26.3%. However, it can be seen that increasing the initial hydrogen pressure does not have any influence on the extent of sulfur removal that was approximately 13.2% for all the range of H_2 initial pressures investigated. The decrease in sulfur content of the produced oil slightly increased from 11.2 to 15.2% as the reaction time increased from Level 1 to Level 4 (20 to 80 min). It was suggested that some of the sulfur in the heavy oil was removed as a result of sulfidation of the iron NPs during reaction and coke deposition.[17] The sulfur content showed an average of 13.2% as the stirring speed increased from Level 1 to Level 4 (200 to 900 rpm) within a standard deviation of ±0.025. Similarly the increase in iron metal loading from Level 1 to Level 4 (0.03 to 0.4 wt %) caused a similar level of sulfur removal (an average of 13.2%) within a standard deviation of ±0.025 in the produced oil relative to the heavy feed oil 3.09 wt %. The above results indicate that the breaking of the C−S bond is largely temperature driven to overcome the bond energy, although the metal loading can influence the interaction with the C−S bond and hydrogen to improve removal.[46]

The removal of metals (i.e., Ni+V) was observed to be 7.6% below the 0.0132 wt % of the feed oil, for the ranges of initial hydrogen pressure, metal loading, stirring speed, and reaction time investigated. Increasing these reaction factors did not have a remarkable effect on the extent of Ni+V removal. However,

DOI: 10.1021/acs.energyfuels.5b01451
Energy Fuels 2015, 29, 6306−6316

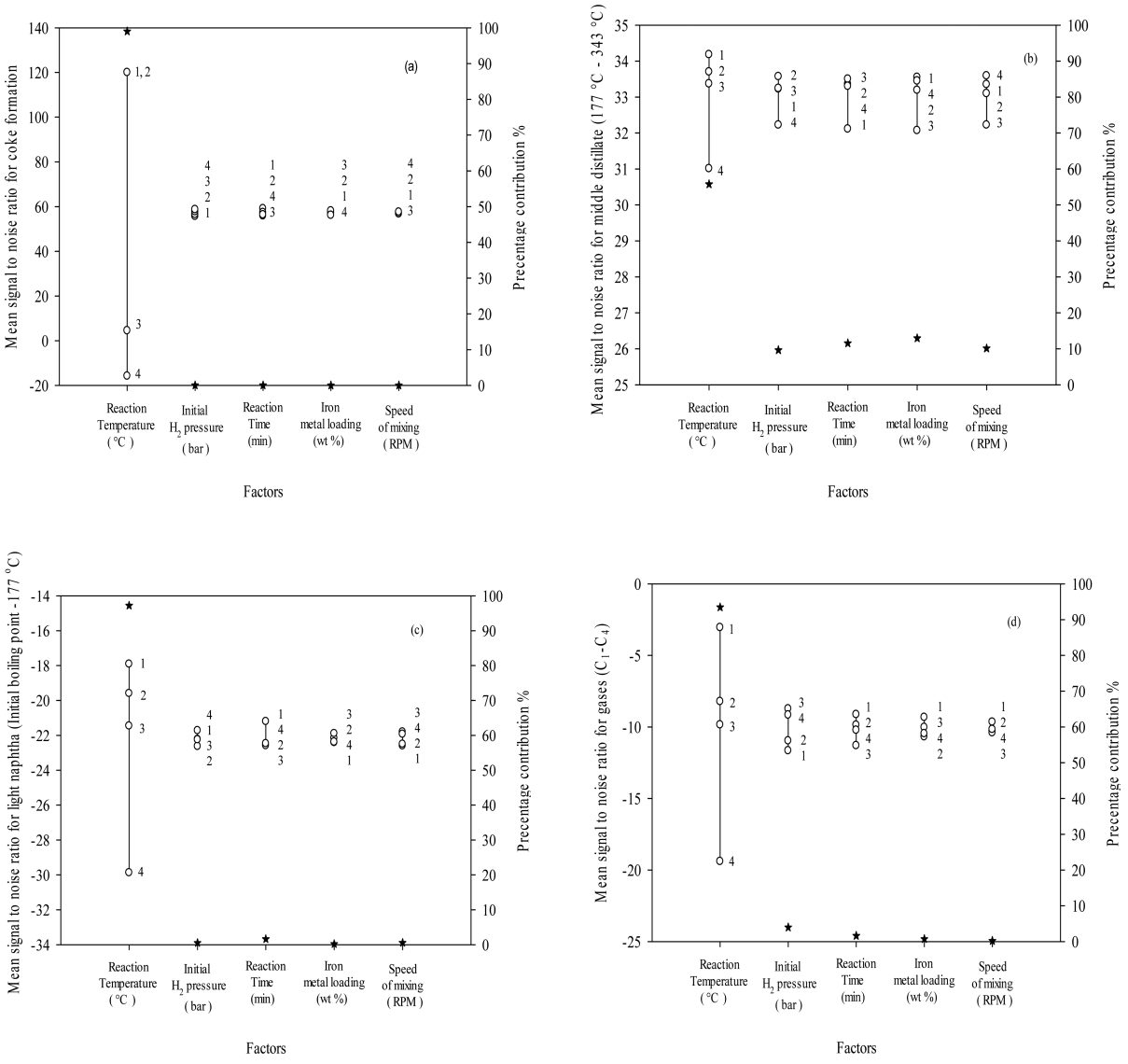

Figure 4. Effect of reaction factors on mean signal-to-noise ratio (a) coke formation (smaller the better) (b) middle distillate (177−343 °C) (larger the better) (c) light naphtha (IBP: 177 °C) (smaller the better) (d) gases (C_1−C_4) (smaller the better). The mean of each factors is indicated by a circle and the number next to each circle indicates the factor level, percentage contribution indicated by an asterisk. For details of reaction factors and their levels and (S/N) ratio calculation, see Tables 2 and 4.

increasing the reaction temperature from Level 1 to Level 4 (355 to 425 °C) increased the removal of Ni+V metals from 7.5 to 68.9% below 0.0132 wt % for the heavy feed oil. The removed metals (Ni+V) are deposited on the NPs and with produced coke as metallic sulfides.[17] In reality, the sulfur and metals removed from the heavy oil will be left behind in the oil reservoir during *in situ* catalytic upgrading.

Hydrogen plays two important roles in metals (V+Ni) removal, which are hydrodemetallization (HDM) and hydrogenation. First hydrogen could help in hydrogenating unsaturated hetroatoms containing compounds such as quinolines and olefins and it also participates to hydrocrack cyclic (saturated and unsaturated) compounds, which produces a metal sulfide and an organic counterpart. In general, high hydrogen pressure observed in this study favored both reaction steps. In addition, the influence of hydrogen pressure as well as catalyst loading on product quality could be properly evaluated at low reaction temperature.[40,51]

3.5. Selection of Optimum Factors Levels. Taguchi suggests analyzing the mean of signal-to-noise ratio as well as mean of response in order to identify the effect of process factors and optimum conditions. The optimum factor levels were selected in this section based on Taguchi method by performing ANOVA on both mean signal-to-noise ratio (S/N) and mean of response in addition to percentage contribution of reaction factors (Section 2.3). The level of significance was measured in terms of percentage contribution.[20,21,52] The percentage contribution of reaction factors, mean signal-to-noise ratio (S/N) and mean of response are presented graphically in Figures 4, 5, 6.

Reaction factors that have a significant effect on mean signal-to-noise ratio (S/N) are classified as control factors.[21,52,53] It has been reported to set the level of this factor equal to the optimum level to minimize process variability.[16,19] Second, to maintain the mean responses on the target value, the Taguchi method suggests using the signal factor. Ideally, the signal factor is the factor that has the most significant effect on mean response with no effect on

DOI: 10.1021/acs.energyfuels.5b01451
Energy Fuels 2015, 29, 6306−6316

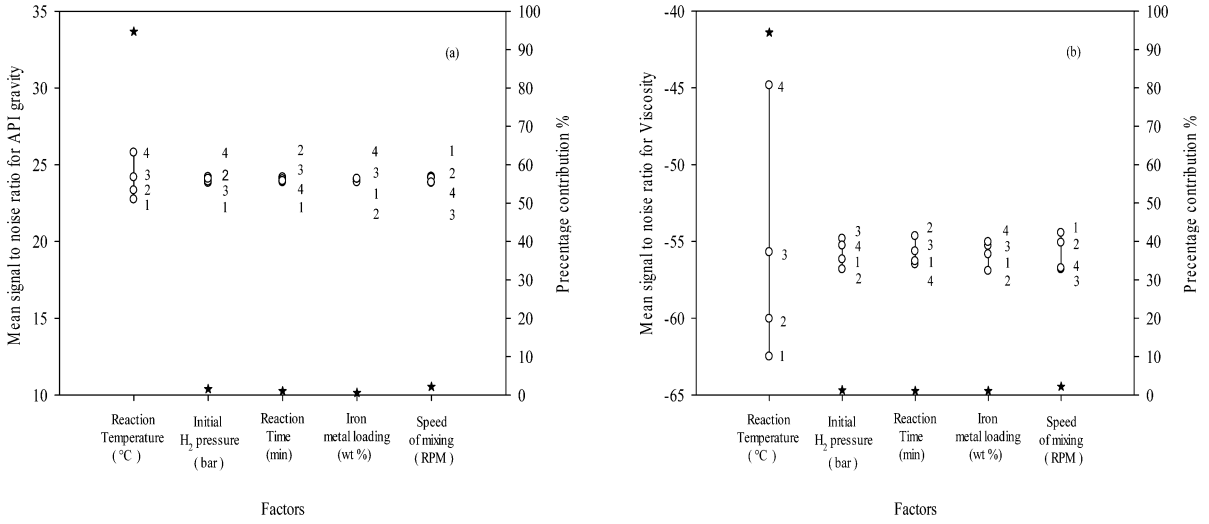

Figure 5. Effect of reaction factors on mean signal-to-noise ratio (a) API gravity (larger the better) (b) viscosity (smaller the better). The mean of each factor is indicated by a circle and the number next to each circle indicates factor level, with percentage contribution indicated by an asterisk. For details of reaction factors and their levels and (S/N) ratio calculation, see Tables 2 and 4.

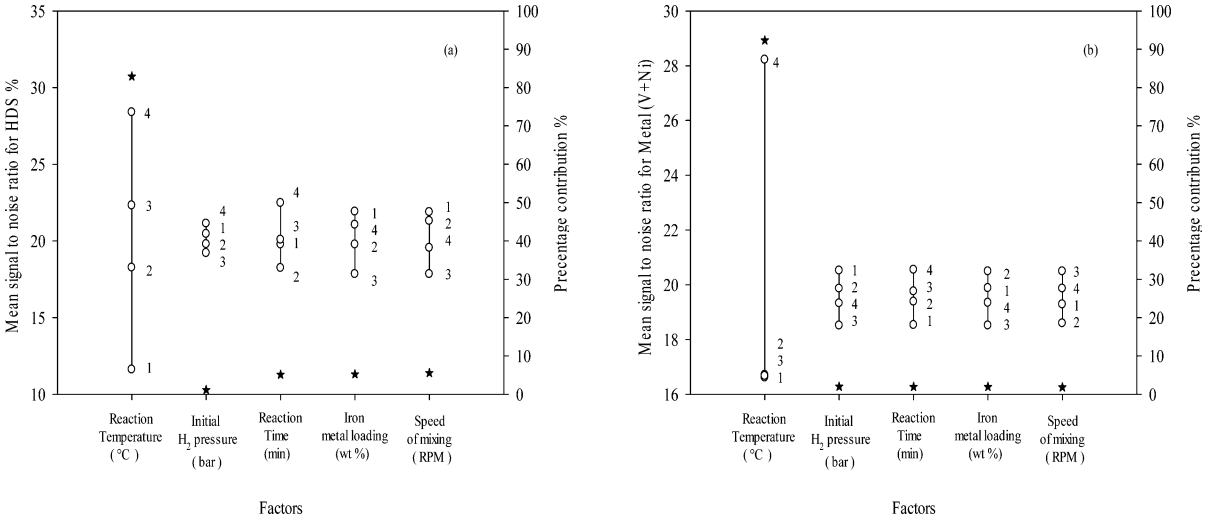

Figure 6. Effect of reaction factors on mean signal-to-noise ratio (a) HDS % (larger the better) (b) metal (V+Ni) (larger the better). The mean of each factor is indicated by a circle and the number next to each circle indicates factor level, with percentage contribution indicated by an asterisk. For details of reaction factors and their levels and (S/N) ratio calculation, see Tables 2 and 4.

the mean S/N of the response. The percentage contribution of the different reaction factors on mean S/N ratio as well as mean of responses can be seen clearly in Figures 4–6, respectively.[18,20,21]

It is clear from the results and Figures 4–6 that reaction temperature has the most significant effect on mean S/N ratio; and hence, is the most important control factor. Also, it is evident that reaction temperature has the most significant effect on the mean of all responses. However, iron–metal loading and initial H_2 pressure have a significant effect on middle distillate fraction and gases, respectively. Among the reaction temperature, iron–metal loading and H_2 initial pressure factors, the reaction temperature is the control factor and so it is not suitable as a signal factor. The remaining two factors, iron–metal loading and initial H_2 pressure, have a moderate effect on middle distillate fraction and gas yields and therefore are assigned as signal factors. Other factors, such as reaction time and mixing speed, could be set at an economical level where they have no significant effect on either the mean S/N ratio or mean of response. In this study, the optimum level of the control factor (reaction temperature), as well as signal factors, were selected and tested, and the results presented in Tables 6 and 7, respectively.

4. CONCLUSION

A comprehensive optimization study has been made of process variable effects of dispersed nanoparticles of iron oxide during THAI–CAPRI *in situ* catalytic upgrading of heavy oil, in a stirred batch reactor. The following process variables reaction temper-

Table 6. Optimum Factor Levels and Conditions

factor	optimum level	selected conditions
reaction temperature (°C)	4	425
initial H_2 pressure (bar)	4	50
reaction time (min)	normal	60
iron metal loading (wt %)	3	0.1
speed of mixing (RPM)	normal	400–600

DOI: 10.1021/acs.energyfuels.5b01451
Energy Fuels 2015, 29, 6306–6316

Table 7. Results of Upgrading Oil at Optimum Conditions

physical properties	value
API° gravity	21.1
viscosity (cP)	105.75
product quality	
HDS%	37.54
metal (Ni+V) wt %	0.062
product distribution	
coke formation wt %	6.79
gases (C_1–C_4) wt %	10.72
naphtha fraction (IBP 177 °C) wt %	21
distillate fraction (177–343 °C) wt %	47

ature, time, initial hydrogen pressure, agitation, and iron metal loading were optimized. At the optimum conditions of 425 °C, 60 min, 400 rpm, 0.1 wt % metal loading, and 50 bar obtained by the Taguchi method, the viscosity reduction was 92.9%, API gravity increased 8.3°, sulfur reduction 37.54%, and metals (Ni +V) reduction 68.9%, relative to the feed oil values, while coke formation was 6.7 wt %. It was also found that the naphtha (IBP: 177 °C) and middle distillate fractions (177–343 °C) at the optimum condition increased from 0.68 and 28.18 wt % in feed oil, to 21 and 47 wt %, respectively in the upgraded oil.

AUTHOR INFORMATION

Corresponding Author

*J. Wood. Tel.: +44 (0) 1214145295. Fax: +44 (0)1214145324. E-mail: J.Wood@bham.ac.uk.

Notes

The authors declare no competing financial interest.

ACKNOWLEDGMENTS

The authors acknowledge the financial support of Kuwait Institute for scientific research KISR, Kuwait, EPSRC (Grant No. EP/E057977/1 and EP/J008303/1), United Kingdom and Petrobank Energy and Resources Ltd. (now Touchstone Exploration Inc.), Canada, for supplying the heavy crude oil used in this study. The sulfur and metals analyses were performed by Warwick Analytical Service University of Warwick Science Park, UK. Datasets regarding this publication are available online free of charge via http://epapers.bham.ac.uk/

REFERENCES

(1) Hart, A.; Leeke, G.; Greaves, M.; Wood, J. Down-hole heavy crude oil upgrading by CAPRI: Effect of hydrogen and methane gases upon upgrading and coke formation. *Fuel* **2014**, *119*, 226–235.

(2) Martínez-Palou, R.; Mosqueira, M. d. L.; Zapata-Rendón, B.; Mar-Juárez, E.; Bernal-Huicochea, C.; de la Cruz Clavel-López, J.; Aburto, J. Transportation of heavy and extra-heavy crude oil by pipeline: A review. *J. Pet. Sci. Eng.* **2011**, *75* (3–4), 274–282.

(3) Dim, P.; Hart, A.; Wood, J.; Macnaughtan, B.; Rigby, S. P. Characterization of pore coking in catalyst for thermal down-hole upgrading of heavy oil. *Chem. Eng. Sci.* **2015**, *131*, 138–145.

(4) Greaves, M.; Dong, L. L.; Rigby, S. P. Simulation study of the Toe-to-Heel Air Injection three-dimensional combustion cell experiment and effects in the mobile oil zone. *Energy Fuels* **2012**, *26* (3), 1656–1669.

(5) Xia, T. X.; Greaves, M. Upgrading Athabasca tar sand using toe-to-heel air injection. *J. Can. Pet. Technol.* **2002**, *41* (8), 51–57.

(6) Hoshyargar, V.; Ashrafizadeh, S. N. Optimization of flow parameters of heavy crude oil-in-water emulsions through pipelines. *Ind. Eng. Chem. Res.* **2013**, *52* (4), 1600–1611.

(7) Hashemi, R.; Nassar, N. N.; Almao, P. P. Enhanced heavy oil recovery by in situ prepared ultradispersed multimetallic nanoparticles: A Study of Hot Fluid Flooding for Athabasca Bitumen Recovery. *Energy Fuels* **2013**, *27* (4), 2194–2201.

(8) Hart, A.; Shah, A.; Leeke, G.; Greaves, M.; Wood, J. Optimization of the CAPRI process for heavy oil upgrading: effect of hydrogen and guard bed. *Ind. Eng. Chem. Res.* **2013**, *52* (44), 15394–15406.

(9) Shah, A.; Fishwick, R.; Wood, J.; Leeke, G.; Rigby, S.; Greaves, M. A review of novel techniques for heavy oil and bitumen extraction and upgrading. *Energy Environ. Sci.* **2010**, *3* (6), 700–714.

(10) Hart, A.; Greaves, M.; Wood, J. A comparative study of fixed-bed and dispersed catalytic upgrading of heavy crude oil using-CAPRI. *Chem. Eng. J.* **2015**, DOI: 10.1016/j.cej.2015.01.101.

(11) Hashemi, R.; Nassar, N. N.; Pereira Almao, P. Nanoparticle technology for heavy oil in-situ upgrading and recovery enhancement: Opportunities and challenges. *Appl. Energy* **2014**, *133*, 374–387.

(12) Krishnamoorti, R. Extracting the benefits of nanotechnology for the oil industry. *JPT, J. Pet. Technol.* **2006**, *58* (11), 24.

(13) Ovalles, C.; Filgueiras, E.; Morales, A.; Scott, C. E.; Gonzalez-Gimenez, F.; Pierre Embaid, B. Use of a dispersed iron catalyst for upgrading extra-heavy crude oil using methane as source of hydrogen. *Fuel* **2003**, *82* (8), 887–892.

(14) Khalil, M.; Lee, R. L.; Liu, N. Hematite nanoparticles in aquathermolysis: A desulfurization study of thiophene. *Fuel* **2015**, *145*, 214–220.

(15) Rezaei, M.; Schaffie, M.; Ranjbar, M. Thermocatalytic in situ combustion: Influence of nanoparticles on crude oil pyrolysis and oxidation. *Fuel* **2013**, *113*, 516–521.

(16) Kowalczyk, M. Application of Taguchi and ANOVA methods in selection of process parameters for surface roughness in precision turning of titanium. *Adv. Manuf. Sci. Technol.* **2014**, *38* (2), 21–35.

(17) Ancheyta, J.; Sánchez, S.; Rodríguez, M. A. Kinetic modeling of hydrocracking of heavy oil fractions: A review. *Catal. Today* **2005**, *109* (1–4), 76–92.

(18) Pignatiello, J. J., Jr Strategies for robust multiresponse quality engineering. *IIE Transactions* **1993**, *25* (3), 5–15.

(19) Fratila, D.; Caizar, C. Application of Taguchi method to selection of optimal lubrication and cutting conditions in face milling of AlMg3. *J. Cleaner Prod.* **2011**, *19* (6–7), 640–645.

(20) Ghani, J. A.; Choudhury, I. A.; Hassan, H. H. Application of Taguchi method in the optimization of end milling parameters. *J. Mater. Process. Technol.* **2004**, *145* (1), 84–92.

(21) Phadke, M. S.; Kackar, R. N.; Speeney, D. V.; Grieco, M. J. Off-line quality control in integrated circuit fabrication using experimental design. *Bell Syst. Tech. J.* **1983**, *62* (5), 1273–1309.

(22) Athreya, S.; Venkatesh, Y. Application of Taguchi method for optimization of process parameters in improving the surface roughness of lathe facing operation. *Int. Refereed J. Eng. Sci.* **2012**, *1* (3), 13–19.

(23) Tansel, I. N.; Gülmez, S.; Demetgul, M.; Aykut, Ş. Taguchi Method–GONNS integration: Complete procedure covering from experimental design to complex optimization. *Expert Syst. Appl.* **2011**, *38* (5), 4780–4789.

(24) Kaneko, T.; Tazawa, K.; Okuyama, N.; Tamura, M.; Shimasaki, K. Effect of highly dispersed iron catalyst on direct liquefaction of coal. *Fuel* **2000**, *79* (3–4), 263–271.

(25) Derbyshire, F.; Hager, G. T. Dispersed catalysts for coal dissolution. *Abstr. Pap. Am. Chem. Soc.* **1992**, *203*, 51-CATL.

(26) Panariti, N.; Del Bianco, A.; Del Piero, G.; Marchionna, M. Petroleum residue upgrading with dispersed catalysts: Part 1. Catalysts activity and selectivity. *Appl. Catal., A* **2000**, *204* (2), 203–213.

(27) Liu, D.; Kong, X.; Li, M. Y.; Que, G. H. Study on a Water-Soluble Catalyst for Slurry-Phase Hydrocracking of an Atmospheric Residue. *Energy Fuels* **2009**, *23* (1), 958–961.

(28) Ren, R.; Wang, Z.; Guan, C.; Shi, B. Study on the sulfurization of molybdate catalysts for slurry-bed hydroprocessing of residuum. *Fuel Process. Technol.* **2004**, *86* (2), 169–178.

(29) Bhattacharyya, A.; Mezza, B. J. Process for using catalyst with rapid formation of iron sulfide in slurry hydrocracking. Patent No. US 8,277,638 B2, October 2, 2012.

DOI: 10.1021/acs.energyfuels.5b01451
Energy Fuels 2015, 29, 6306–6316

(30) Angeles, M. J.; Leyva, C.; Ancheyta, J.; Ramírez, S. A review of experimental procedures for heavy oil hydrocracking with dispersed catalyst. *Catal. Today* **2014**, *220*−*222*, 274−294.
(31) Speight, J. *Chapter 5: Thermal cracking the refinery of the future, and hydrotreating (HDT)* **2011**, 147−180.
(32) Rana, M. S.; Sámano, V.; Ancheyta, J.; Diaz, J. A. I. A review of recent advances on process technologies for upgrading of heavy oils and residua. *Fuel* **2007**, *86* (9), 1216−1231.
(33) Fujimoto, K.; Chang, J.; Tsubaki, N. Hydrothermal cracking of residual oil. *Sekiyu Gakkaishi* **2000**, *43* (1), 25−36.
(34) Del Bianco, A.; Panariti, N.; Di Carlo, S.; Beltrame, P. L.; Carniti, P. New developments in deep hydroconversion of heavy oil residues with dispersed catalysts. 2. Kinetic aspects of reaction. *Energy Fuels* **1994**, *8* (3), 593−597.
(35) Elizalde, I.; Rodríguez, M. A.; Ancheyta, J. Modeling the effect of pressure and temperature on the hydrocracking of heavy crude oil by the continuous kinetic lumping approach. *Appl. Catal., A* **2010**, *382* (2), 205−212.
(36) Elizalde, I.; Rodríguez, M. A.; Ancheyta, J. Application of continuous kinetic lumping modeling to moderate hydrocracking of heavy oil. *Appl. Catal., A* **2009**, *365* (2), 237−242.
(37) Liu, D.; Li, M. Y.; Deng, W. A.; Que, G. H. Reactivity and composition of dispersed Ni catalyst for slurry-phase residue hydrocracking. *Energy Fuels* **2010**, *24*, 1958−1962.
(38) Il Yoon, Y.; Wook Kim, M.; Seung Yoon, Y.; Kim, S. H. A kinetic study on medium temperature desulfurization using a natural manganese ore. *Chem. Eng. Sci.* **2003**, *58* (10), 2079−2087.
(39) Fixari, B.; Peureux, S.; Elmouchnino, J.; Le Perchec, P.; Vrinat, M.; Morel, F. New developments in deep hydroconversion of heavy oil residues with dispersed catalysts. 1. Effect of metals and experimental conditions. *Energy Fuels* **1994**, *8* (3), 588−592.
(40) Panariti, N.; Del Bianco, A.; Del Piero, G.; Marchionna, M.; Carniti, P. Petroleum residue upgrading with dispersed catalysts: Part 2. Effect of operating conditions. *Appl. Catal., A* **2000**, *204* (2), 215−222.
(41) Bellussi, G.; Rispoli, G.; Landoni, A.; Millini, R.; Molinari, D.; Montanari, E.; Moscotti, D.; Pollesel, P. Hydroconversion of heavy residues in slurry reactors: Developments and perspectives. *J. Catal.* **2013**, *308*, 189−200.
(42) Weitkamp, J. Catalytic Hydrocracking—Mechanisms and Versatility of the Process. *ChemCatChem* **2012**, *4* (3), 292−306.
(43) Kennepohl, D.; Sanford, E. Conversion of Athabasca bitumen with dispersed and supported Mo-based catalysts as a function of dispersed catalyst concentration. *Energy Fuels* **1996**, *10* (1), 229−234.
(44) Dabkowski, M. J.; Shih, S. S.; Albinson, K. R. Upgrading of petrolume residue with dispresed additive. *Am. Inst. Chem. Eng.*; AIChE: New York, 1991; Vol. *87*, pp 53−61.
(45) Luo, H.; Deng, W. N.; Gao, J. J.; Fan, W. Y.; Que, G. H. Dispersion of water-soluble catalyst and its influence on the slurry-phase hydrocracking of residue. *Energy Fuels* **2011**, *25* (3), 1161−1167.
(46) Gray, M. R. *Upgrading petroleum residues and heavy oil*, 1st ed.; CRC Press: Boca Raton, FL, 1994.
(47) Rezaei, H.; Ardakani, S. J.; Smith, K. J. Comparison of MoS_2 catalysts prepared from Mo-micelle and Mo-octoate precursors for hydroconversion of Cold Lake vacuum residue: catalyst activity, coke properties and catalyst recycle. *Energy Fuels* **2012**, *26* (5), 2768−2778.
(48) Zhang, H. Q.; Sarica, C.; Pereyra, E. Review of high-viscosity oil multiphase pipe flow. *Energy Fuels* **2012**, *26* (7), 3979−3985.
(49) Sambi, I. S.; Khulbe, K. C.; Mann, R. S. Catalytic hydrotreatment of heavy gas oil. *Ind. Eng. Chem. Prod. Res. Dev.* **1982**, *21* (4), 575−580.
(50) Jafari, R.; Chaouki, J.; Tanguy, P. A. A Comprehensive review of just suspended speed in liquid-solid and gas-liquid-solid stirred tank reactors. *Int. J. Chem. React. Eng.* **2012**, *10*, DOI: 10.1515/1542-6580.2808.
(51) Reynolds, J. G. Modeling hydrodesulfurization, hydrodentrification and hydrodemetalation. *Chem. Ind.* **1991**, *16*, 570−574.
(52) Kolahan, F.; Manoochehri, M.; Hosseini, A. Application of Taguchi method and ANOVA analysis for simultaneous optimization of machining parameters and tool geometry in turning. *International Conference on Computer, Electrical and Systems Science and Engineering*, Bali, Indonesia, October 26−28, 2011.
(53) Simpson, J. R. Robust design and analysis for quality engineering. *J. Qual. Technol.* **1998**, *30* (2), 182.

DOI: 10.1021/acs.energyfuels.5b01451
Energy Fuels 2015, 29, 6306−6316